

Screening for lipid nanoparticles that modulate the immune activity of helper T cells towards enhanced antitumour activity

In the format provided by the authors and unedited

Contents

Supplementary Fig. 1 | Z-average size and zeta potential of top seven LNP formulations measured by DLS.

Supplementary Fig. 2 | Detailed analysis to elucidate mRNA/LNP formulation design principles for DC2.4 Transfection *in vitro*.

Supplementary Fig. 3 | Representative flow cytometry plots for *in vivo* assessments of lymph node cell transfection by top LNP formulations.

Supplementary Fig. 4 | Gating strategy for flow cytometry plots for *in vivo* assessments of lymph node cell transfection by top LNP formulations.

Supplementary Fig. 5 | Representative flow cytometry plots for analysis of SIINFEKL-H-2Kb⁺ and CD11c⁺ cells on day 3 post administration.

Supplementary Fig. 6 | Gating strategy for flow cytometry plots for DC antigen presentation and maturation level in dLNs.

Supplementary Fig. 7 | Representative flow cytometry plots for analysis of CD3⁺CD8⁺IFN- γ ⁺ cells.

Supplementary Fig. 8 | Representative flow cytometry plots for analysis of CD3⁺CD8⁺TNF- α ⁺ cells.

Supplementary Fig. 9 | Representative flow cytometry plots for analysis of CD3⁺CD8⁺GranzymeB⁺ cells.

Supplementary Fig. 10 | Gating strategy for flow cytometry plots for cytotoxic T cell response after vaccination.

Supplementary Fig. 11 | Representative flow cytometry plots for analysis of CD3⁺CD4⁺IFN- γ ⁺T-bet⁺ cells.

Supplementary Fig. 12 | Gating strategy for analysis of CD3⁺CD4⁺IFN- γ ⁺T-bet⁺ cells.

Supplementary Fig. 13 | Representative images of IFN- γ secreting cells from the enzyme-linked immunospot assay.

Supplementary Fig. 14 | Gating strategy and representative flow cytometry plots for analysis of CD3⁺CD4⁺IL-4⁺GATA-3⁺ cells.

Supplementary Fig. 15 | Intracellular staining results for antigen specific CD3⁺CD4⁺IL-17⁺ROR γ t⁺ splenocytes from vaccinated mice.

Supplementary Fig. 16 | Gating strategy and representative flow cytometry plots for analysis of CD3⁺CD4⁺IL-17⁺ROR γ t⁺ cells.

Supplementary Fig. 17 | Body weights of mice vaccinated with mOVA-loaded C10, D6, or F5 LNPs.

Supplementary Fig. 18 | Cytokine levels in blood serum samples collected on day 21 from mice vaccinated with different formulations.

Supplementary Fig. 19 | Anti-tumor efficacy of top mRNA LNP formulations as therapeutic vaccines for MC38-OVA tumor model.

Supplementary Fig. 20 | Anti-tumor efficacy of top mRNA LNP formulations as therapeutic vaccines for EG7-OVA tumor model.

Supplementary Fig. 21 | *In vivo* transfection efficiency of LNP formulations in local injection site and major organs.

Supplementary Fig. 22 | Makeup of transfected cells at the injection sites of mice at 24 h post-treatment.

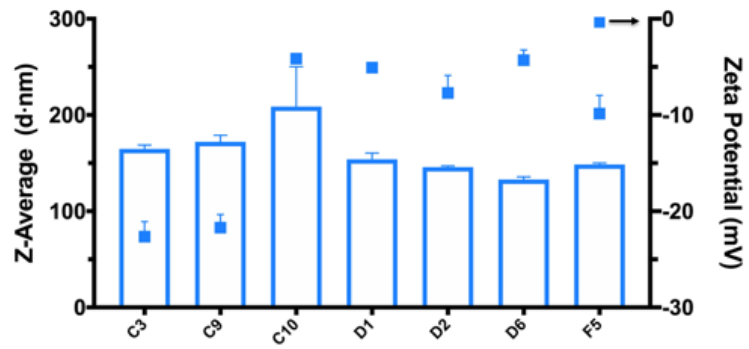
Supplementary Fig. 23 | Representative Z-average diameter distributions measured by DLS of the top 3 mOVA LNP formulations synthesized via larger-scale and small-scale methods.

Supplementary Fig. 24 | Z-average size and zeta potential measurements measured by DLS of the top 3 LNP formulations synthesized via larger-scale and small-scale methods.

Supplementary Fig. 25 | Encapsulation efficiency assessments of the top 3 LNP formulations synthesized via larger-scale and small-scale methods.

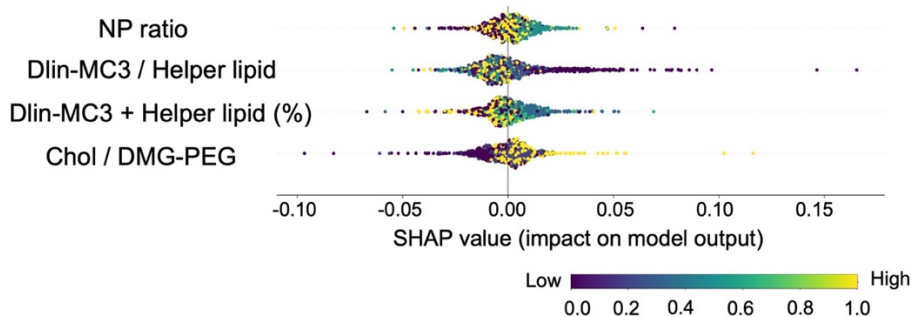
Table 1 | Formulation details for the top 49 LNPs.

Table 2 | Formulation details and particle sizes for the top 7 LNPs.

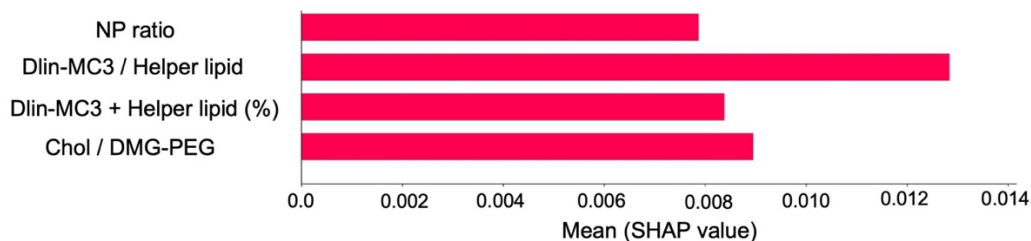


Supplementary Fig. 1 | Z-average size and zeta potential of top seven LNP formulations measured by DLS (n = 3). Zeta potential was shown in cube at right axis. Data are presented as mean \pm S.D. See Supplemental Table 2 for composition details of the selected LNP formulations.

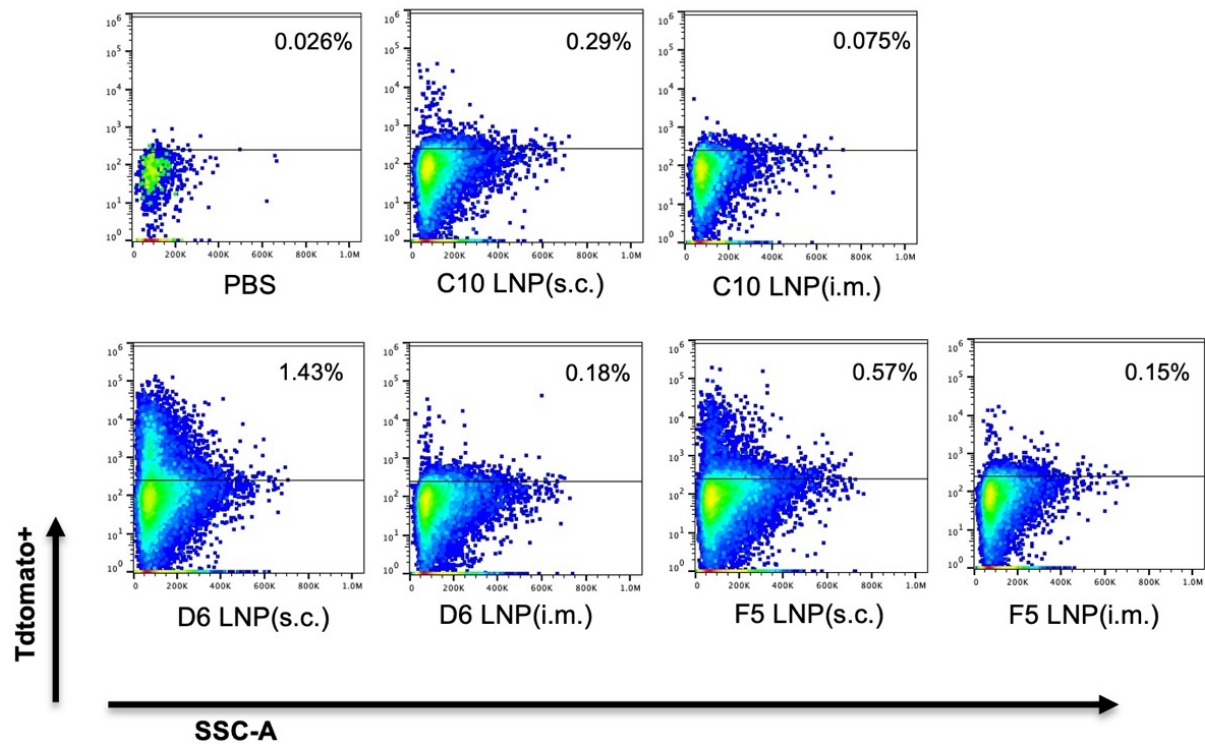
A. SHAP Summary Plot of LGBM Model Features



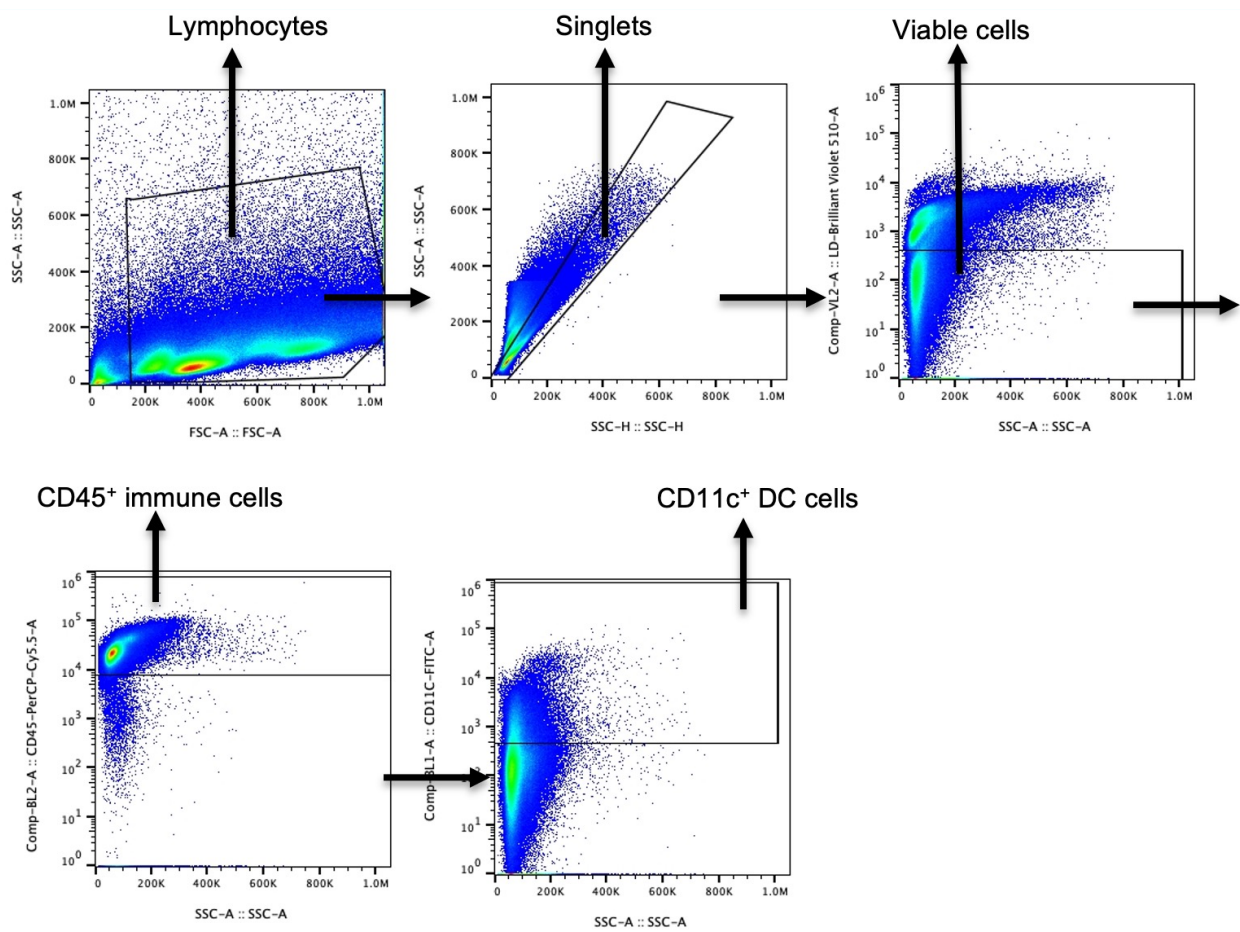
B. SHAP LGBM Feature Importance



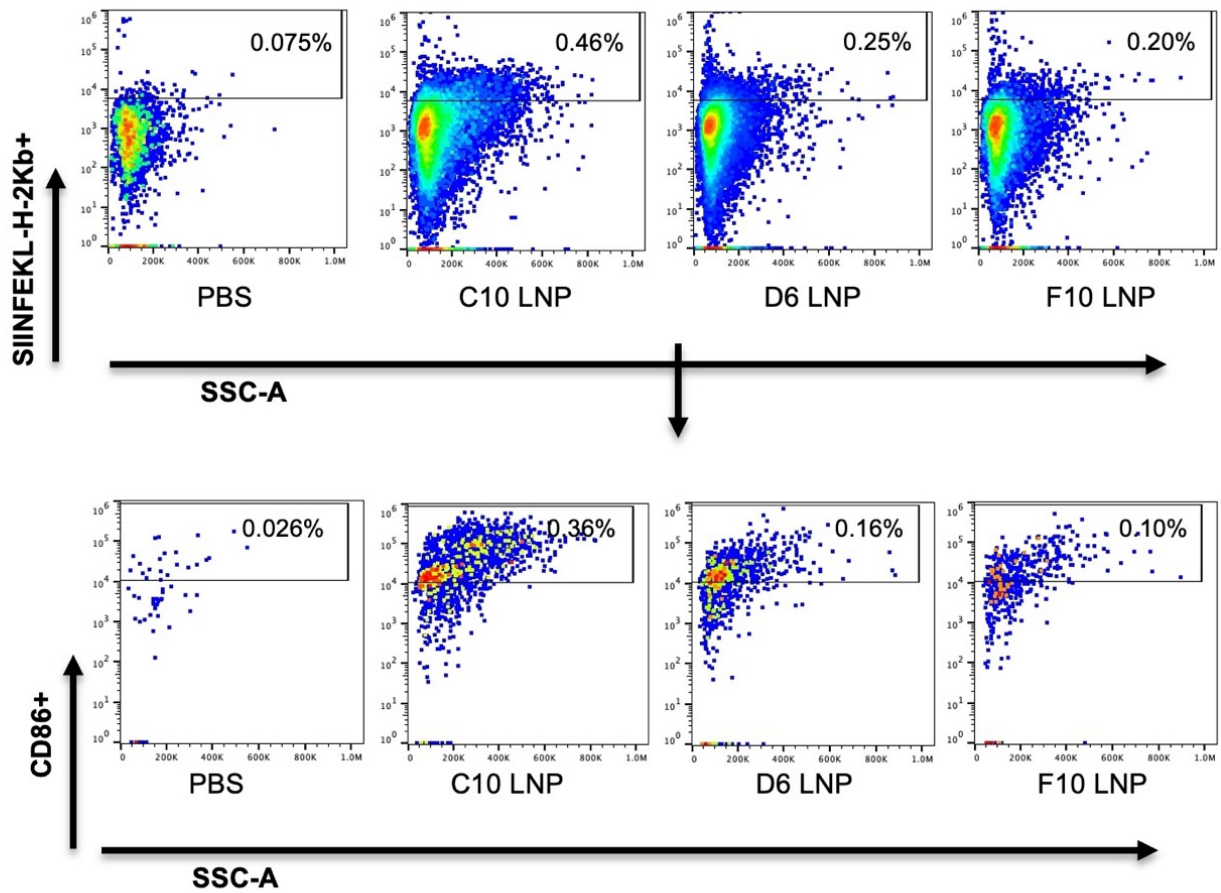
Supplementary Fig. 2 | Detailed analysis to elucidate mRNA/LNP formulation design principles for DC2.4 cell transfection *in vitro*. (A) Optimized LightGBM model Shapley additive explanations (SHAP) analysis summary plot. The impact of formulation parameters on DC2.4 transfection *in vitro* are illustrated through a beeswarm plot of their corresponding SHAP values. The color of the dot represents the relative feature value (normalized within the feature) in the corresponding LNP. The position of the points on the x-axis indicates whether the feature value contributed positively (right) or negatively (left) and the magnitude of the contribution to the predicted transfection of the formulation. (B) Bar plot of the importance of the features to the machine learning transfection predictions based on the mean absolute SHAP value across the dataset.



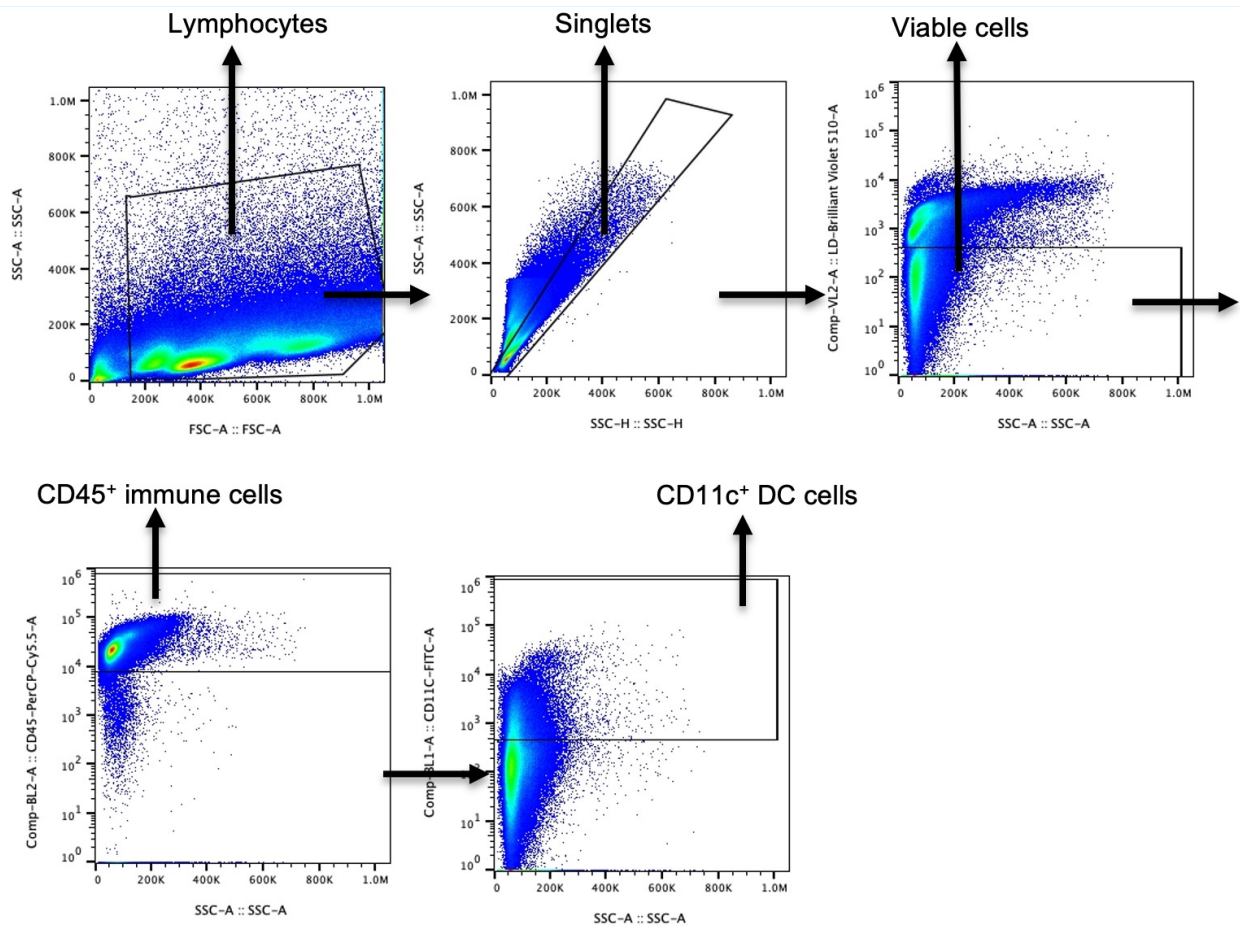
Supplementary Fig. 3 | Representative flow cytometry plots for *in vivo* assessments of lymph node cell transfection by top LNP formulations. Ai9 mice were administered the top three LNPs loaded with mCre via *i.m.* and *s.c.* injections (n = 4, 10 μ g mCre per mouse). Transfection of immune cells in draining lymph nodes was analyzed by flow cytometry. Percentages of cells positive for tdTomato and CD11c gated on CD45⁺ cells are shown. Gating strategy is shown in Supplemental Fig. 5.



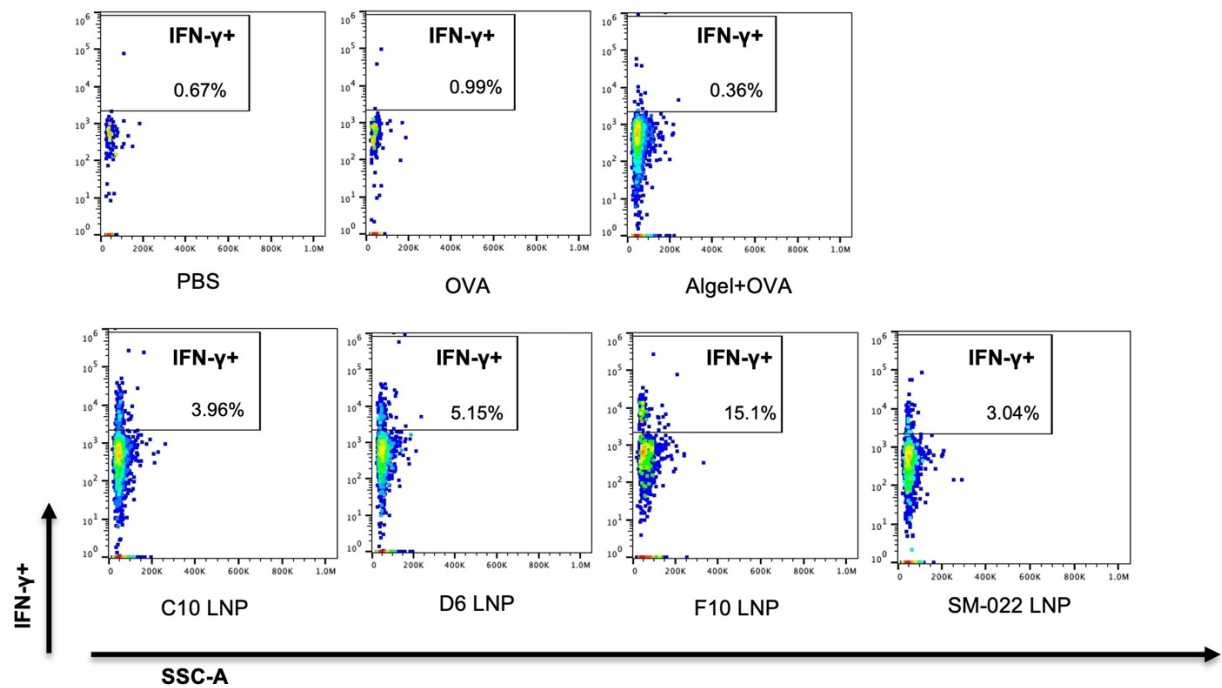
Supplementary Fig. 4 | Gating strategy for flow cytometry plots for *in vivo* assessments of lymph node cell transfection by top LNP formulations. Initially, lymphocytes were selected using SSC-A and FSC-A parameters. Subsequently, singlet cells were selected using the FSC-H and FSC-A plot. Viable cells were identified and selected based on the live/dead Fixable Aqua-A and SSC-A plot. Finally, the CD45⁺ and CD11c⁺ cell populations were selected with subsequent analysis focused on tdTomato signal, as illustrated in representative figures.



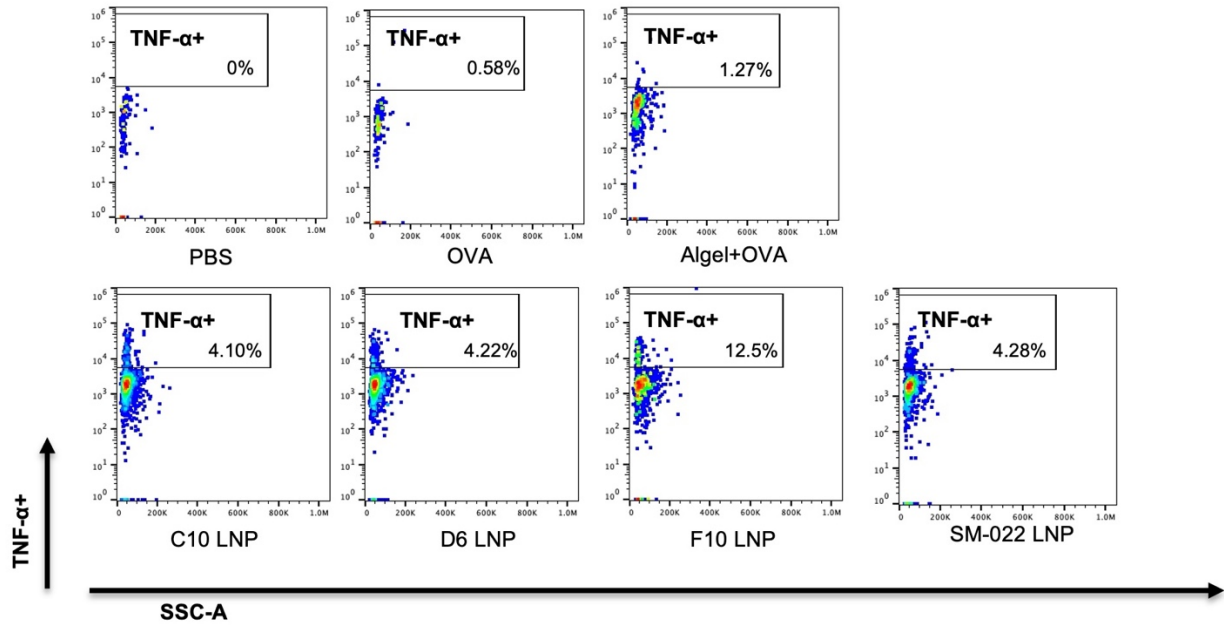
Supplementary Fig. 5 | Representative flow cytometry plots for analysis of SIINFEKL-H-2Kb+ and CD11c+ cells on day 3 post administration. C57BL/6 mice were given one s.c. injection of PBS, C10, D6, or F5 LNPs loaded with mOVA (10 μ g mOVA per injection). Mice were sacrificed three days after the injection, and their lymphocytes in dLNs were isolated for analysis. DC antigen presentation in the draining lymph nodes were analyzed through flow cytometry. Cells positive for CD11c, SIINFEKL-H-2Kb and CD86 are shown.



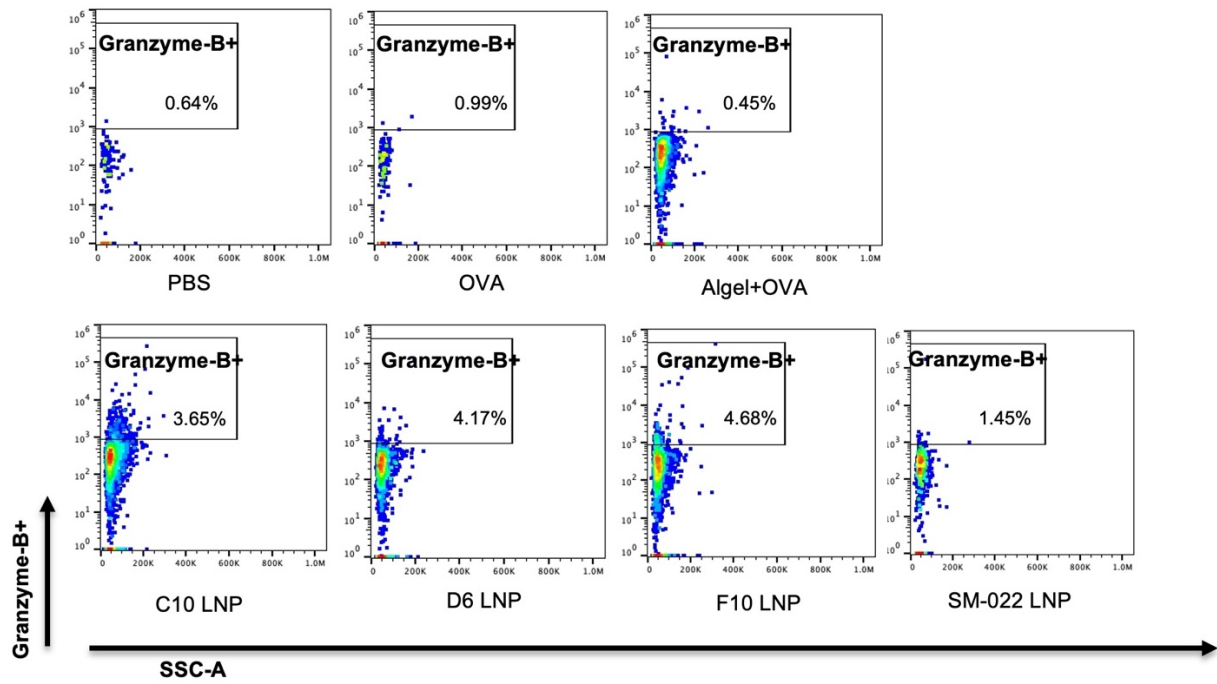
Supplementary Fig. 6 | Gating strategy for flow cytometry plots for DC antigen presentation and maturation level in dLNs. Initially, lymphocytes were gated out using SSC-A and FSC-A parameters. Subsequently, singlet cells were gated out using the FSC-H and FSC-A plot. Viable cells were identified and gated out based on the live/dead Fixable Aqua-A and SSC-A plot. Next, the CD45⁺ and CD11c⁺ cell populations were further gated out. Finally, the analysis focused on SIINFEKL-H-2Kb and CD86, as illustrated in representative figures.



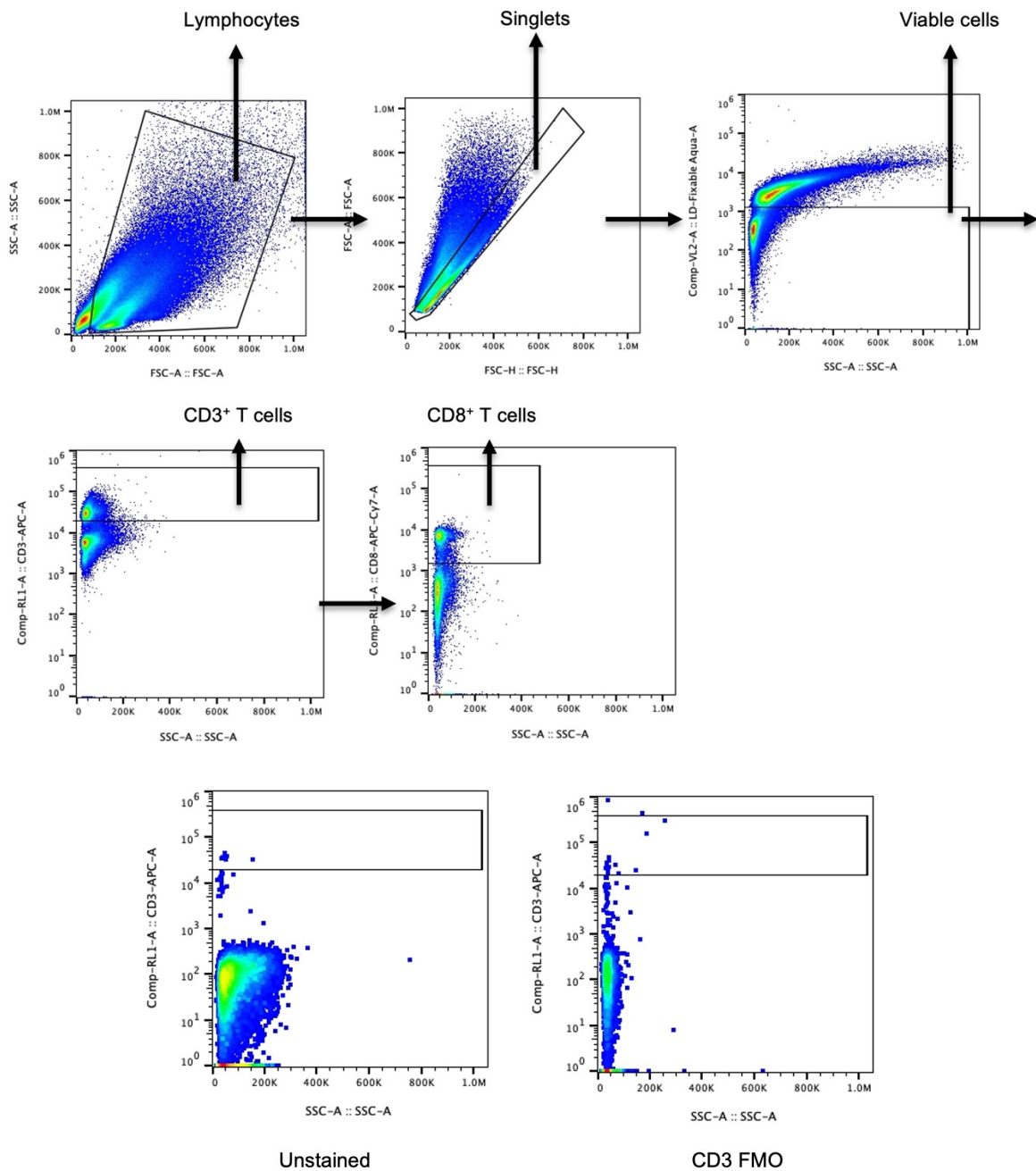
Supplementary Fig. 7 | Representative flow cytometry plots for analysis of CD3⁺CD8⁺IFN- γ ⁺ cells. Splenocytes from mice vaccinated with the displayed formulations were restimulated *in vitro* with OVA and SIINFEKL peptide (100 $\mu\text{g ml}^{-1}$ OVA and 2 $\mu\text{g ml}^{-1}$ SIINFEKL) for 6 h and assessed via FACS and intracellular cytokine staining to determine the percentages of CD3⁺CD8⁺IFN- γ ⁺ cells.



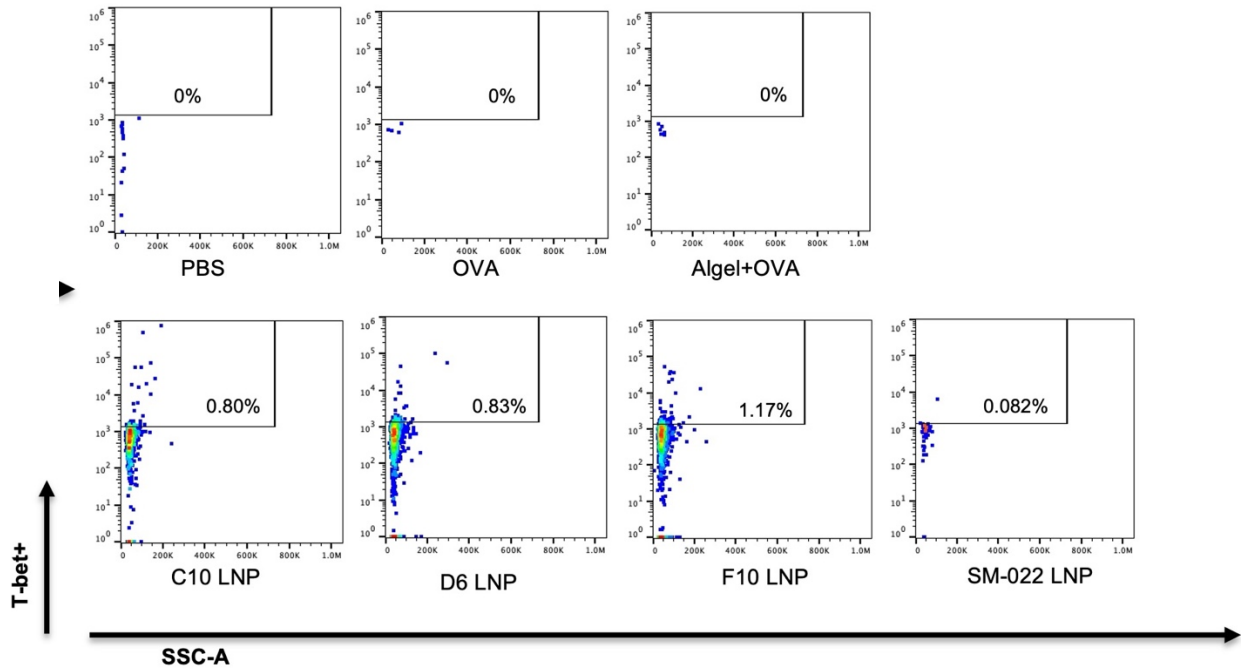
Supplementary Fig. 8 | Representative flow cytometry plots for analysis of CD3⁺CD8⁺TNF- α ⁺ cells. Splenocytes from mice vaccinated with the displayed formulations were restimulated *in vitro* with OVA and SIINFEKL peptide (100 $\mu\text{g ml}^{-1}$ OVA and 2 $\mu\text{g ml}^{-1}$ SIINFEKL) for 6 h and assessed via FACS and intracellular cytokine staining to determine the percentages of CD3⁺CD8⁺TNF- α ⁺ cells.



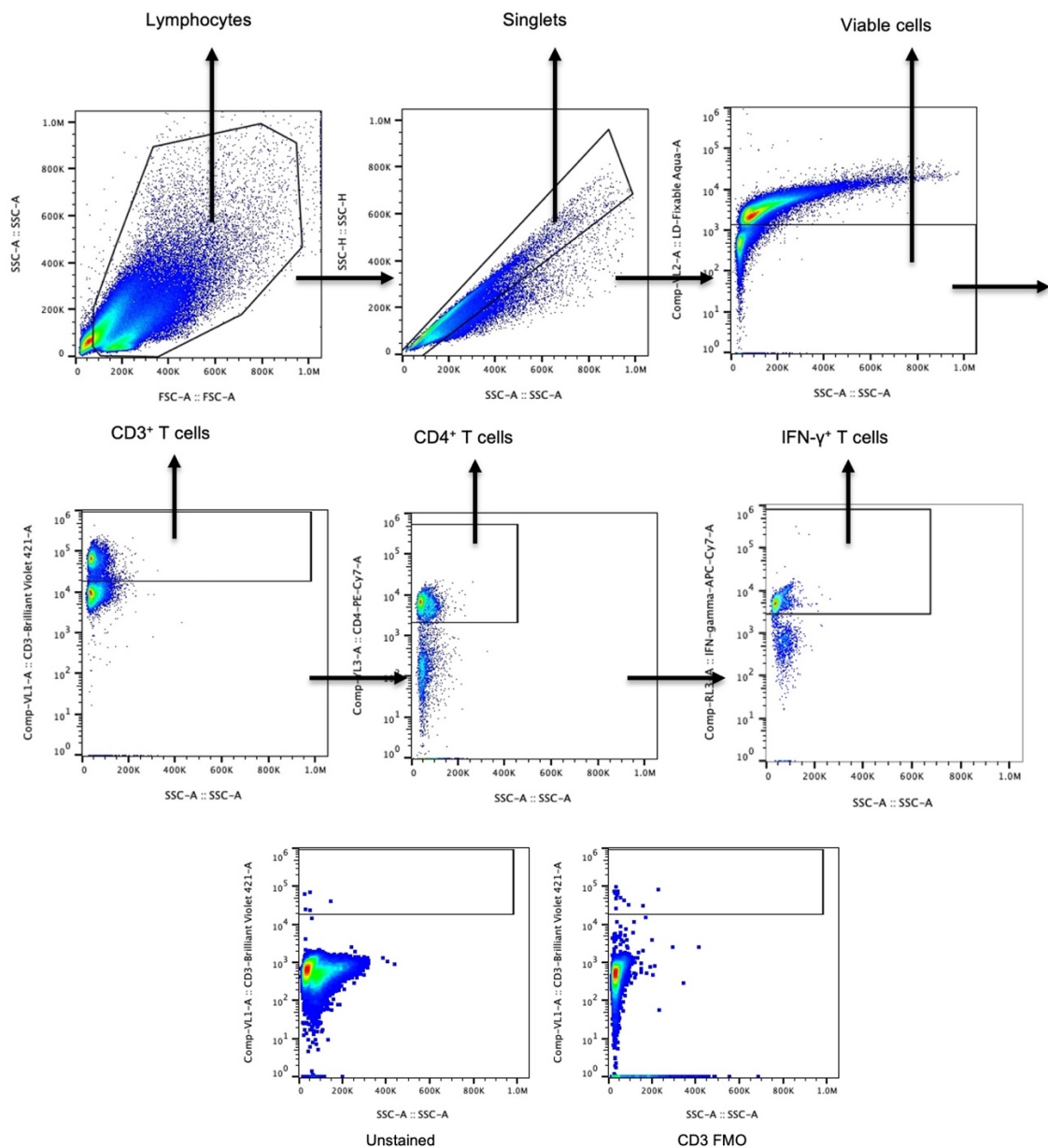
Supplementary Fig. 9 | Representative flow cytometry plots for analysis of CD3⁺CD8⁺GranzymeB⁺ cells. Splenocytes from mice vaccinated with the displayed formulations were restimulated *in vitro* with OVA and SIINFEKL peptide (100 $\mu\text{g ml}^{-1}$ OVA and 2 $\mu\text{g ml}^{-1}$ SIINFEKL) for 6 h and assessed via FACS and intracellular cytokine staining to determine the percentages of CD3⁺CD8⁺Granzyme B⁺ cells.



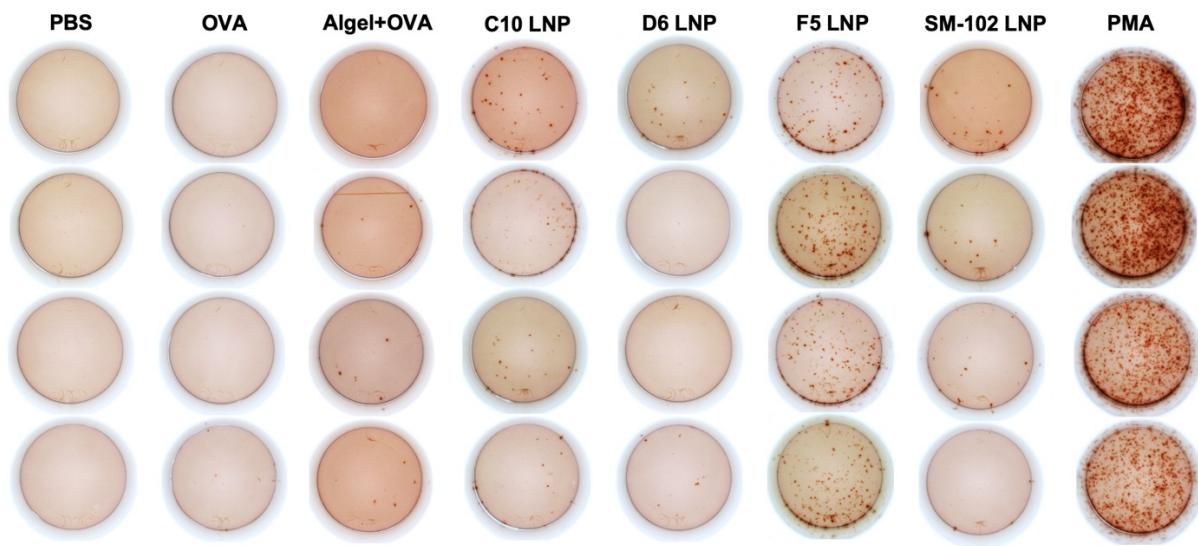
Supplementary Fig. 10 | Gating strategy for flow cytometry plots for cytotoxic T cell response after vaccination. Initially, lymphocytes from the spleen were selected using SSC-A and FSC-A parameters and then singlet cells by FSC-H and FSC-A plot. Viable cells were identified and selected based on the live/dead Fixable Aqua-A and SSC-A plot. Next, the CD3⁺ and CD8⁺ cell populations were selected with downstream analysis focused on IFN- γ , TNF- α , and Granzyme B, as illustrated in the representative figures. The “Unstained” and “CD3 FMO (Fluorescence Minus One)” controls for CD3 T cell gating are included as references.



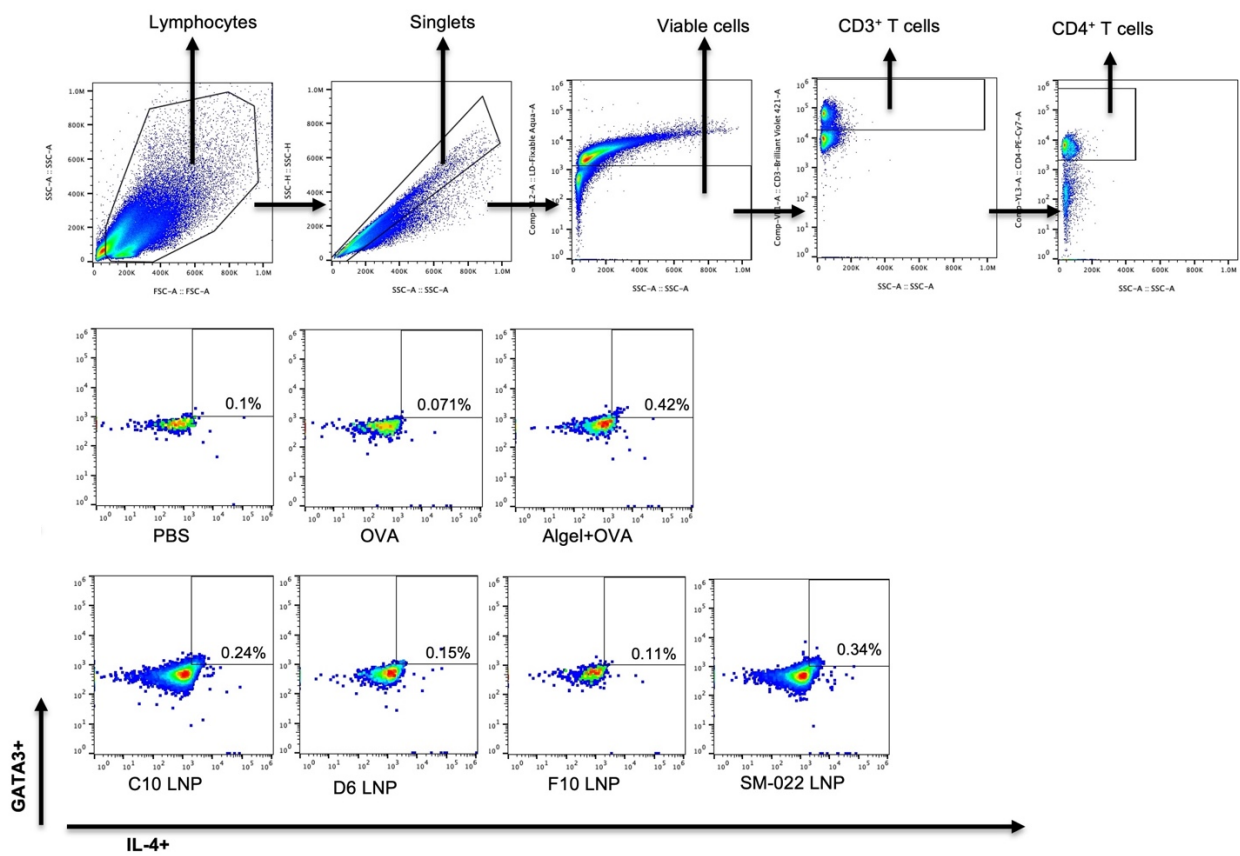
Supplementary Fig. 11 | Representative flow cytometry plots for analysis of CD3⁺CD4⁺IFN- γ ⁺T-bet⁺ cells. Splenocytes from mice vaccinated with the displayed formulations were restimulated *in vitro* with OVA and SIINFEKL peptide (100 μ g ml⁻¹ OVA and 2 μ g ml⁻¹ SIINFEKL) for 6 h and assessed via FACS and intracellular cytokine staining to determine the percentages of CD3⁺CD4⁺IFN- γ ⁺T-bet⁺ cells.



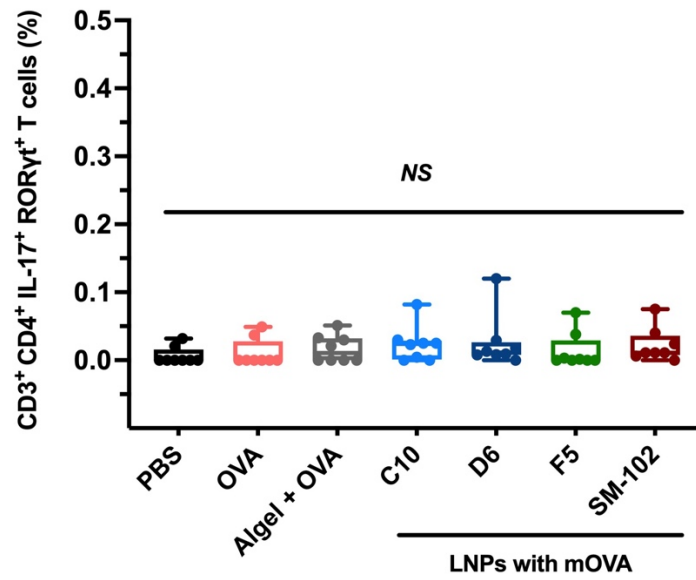
Supplementary Fig. 12 | Gating strategy for analysis of CD3⁺CD4⁺IFN- γ ⁺T-bet⁺ cells. Initially, lymphocytes from the spleen were selected using SSC-A and FSC-A parameters and then singlet cells by FSC-H and FSC-A plot. Viable cells were identified and selected based on the live/dead Fixable Aqua-A and SSC-A plot. Next, the CD3⁺, CD4⁺ and IFN- γ ⁺ cell populations were selected with downstream analysis focused on T-bet, as illustrated in representative figures. The “Unstained” and “CD3 FMO” controls for CD3 T cell gating were included as references.



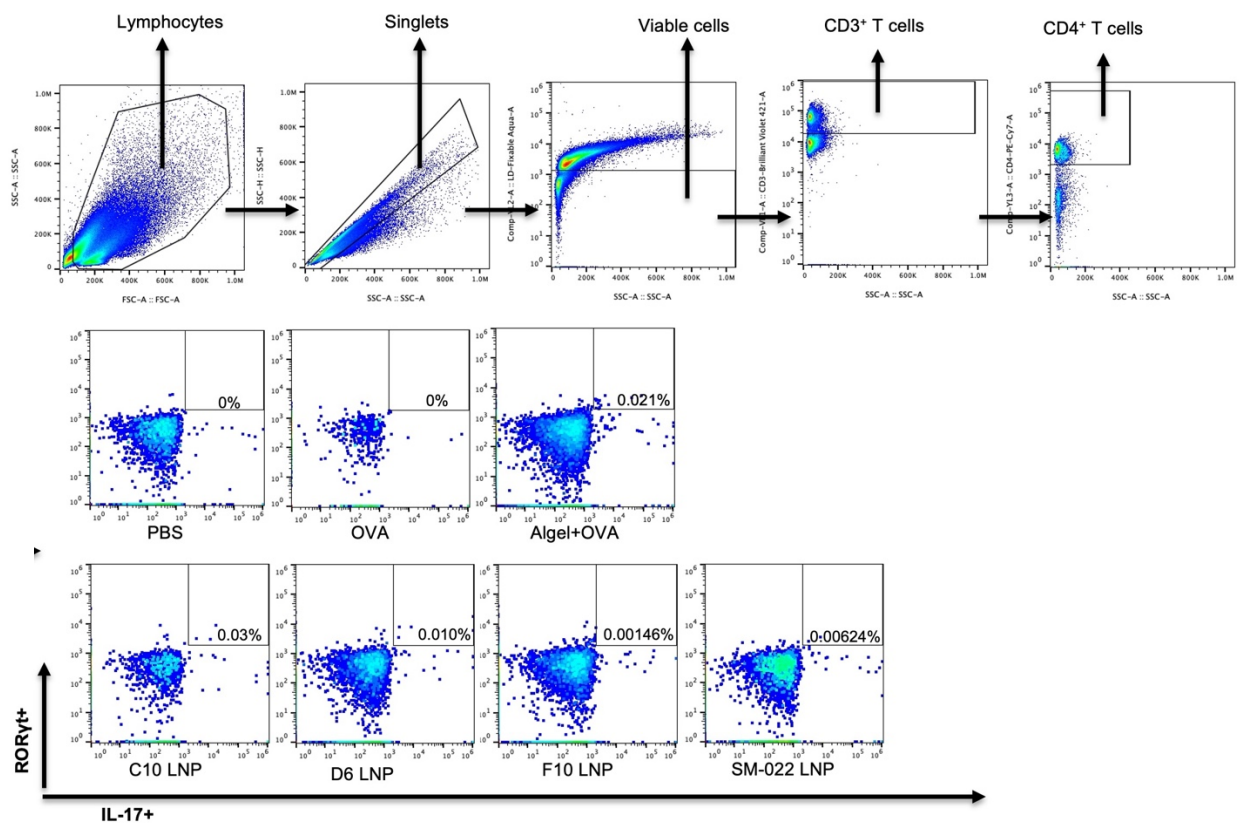
Supplementary Fig. 13 | Representative images of IFN- γ secreting cells from the enzyme-linked immunospot assay. Frequency of IFN- γ -producing cells among restimulated splenocytes, assessed via ELISPOT. Splenocytes were restimulated *in vitro* with SIINFEKL peptide ($2 \mu\text{g ml}^{-1}$ SIINFEKL) for 24 h. 'Algel+OVA' stands for Alhydrogel[®]+OVA group.



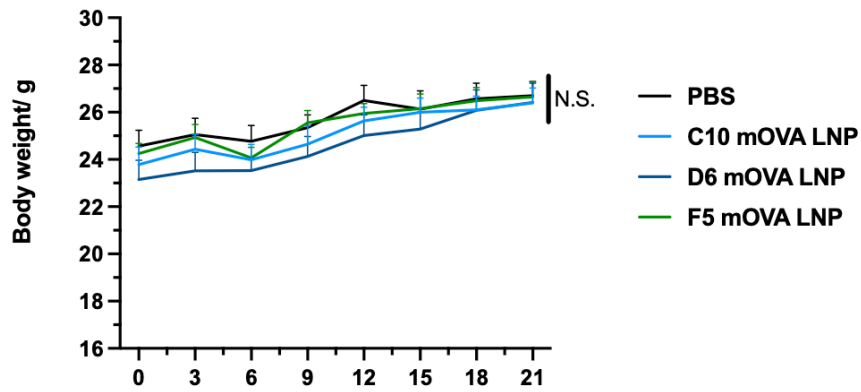
Supplementary Fig. 14 | Gating strategy and representative flow cytometry plots for analysis of CD3⁺CD4⁺IL-4⁺GATA-3⁺ cells. Splenocytes from mice vaccinated with the displayed formulations were restimulated *in vitro* with OVA and SIINFEKL peptide (100 $\mu\text{g ml}^{-1}$ OVA and 2 $\mu\text{g ml}^{-1}$ SIINFEKL) for 6 h and assessed via FACS and intracellular cytokine staining to determine the percentages of CD3⁺CD4⁺IL-4⁺GATA-3⁺ cells.



Supplementary Fig. 15 | Intracellular staining results for antigen specific CD3⁺CD4⁺IL-17⁺RORyt⁺ Th17-type splenocytes from vaccinated mice. Splenocytes from mice vaccinated with the displayed formulations were restimulated in vitro with OVA and SIINFEKL peptide (100 µg ml⁻¹ OVA and 2 µg ml⁻¹ SIINFEKL) for 6 h and assessed via flow cytometry and intracellular cytokine staining to determine the percentages of CD3⁺CD4⁺IL-17⁺RORyt⁺.

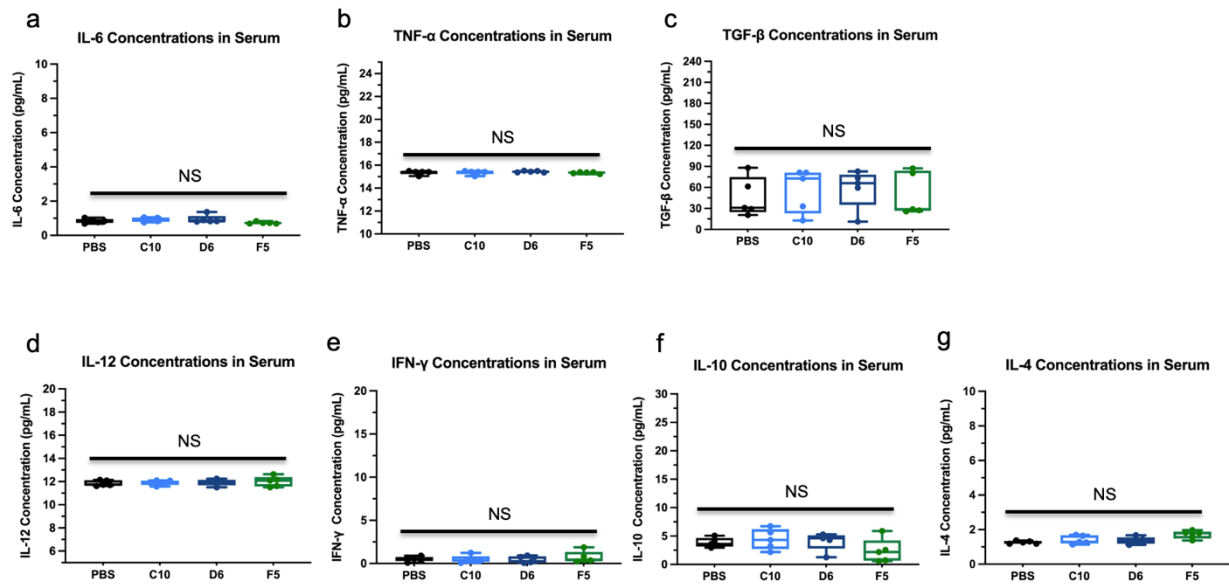


Supplementary Fig. 16 | Gating strategy and representative flow cytometry plots for analysis of CD3⁺CD4⁺IL-17⁺RORyt⁺ cells. Splenocytes from mice vaccinated with the displayed formulations were restimulated *in vitro* with OVA and SIINFEKL peptide (100 $\mu\text{g mL}^{-1}$ OVA and 2 $\mu\text{g mL}^{-1}$ SIINFEKL) for 6 h and assessed via FACS and intracellular cytokine staining to determine the percentages of CD3⁺CD4⁺IL-17⁺RORyt⁺ cells.

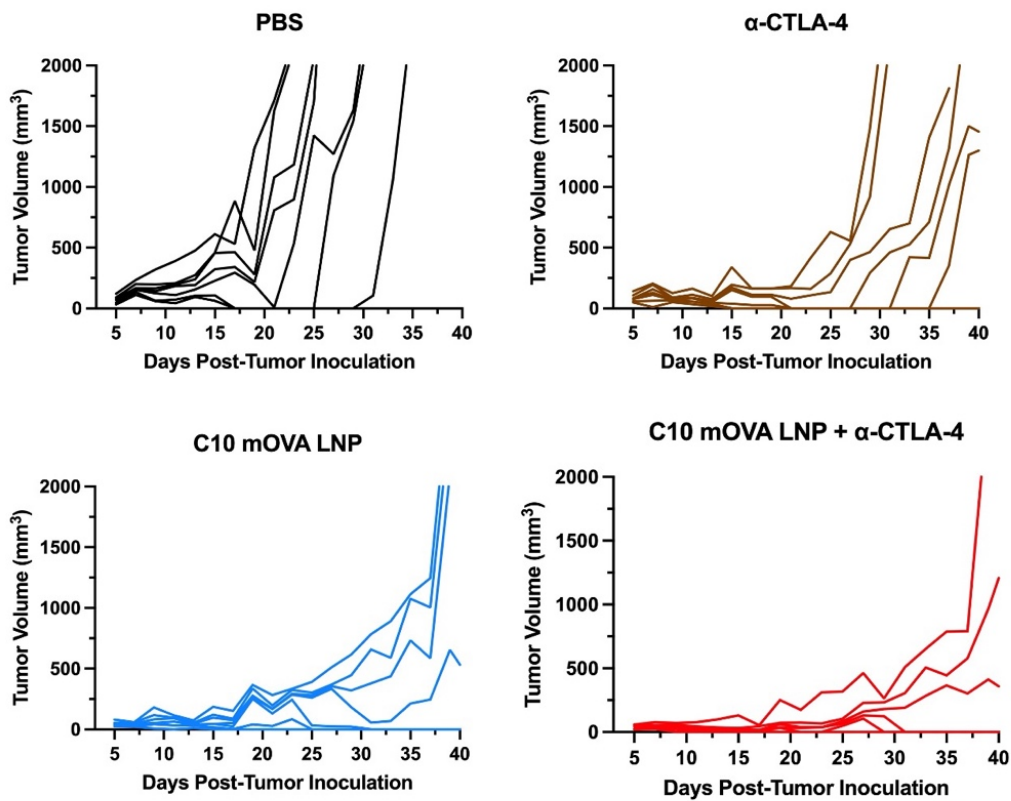


Supplementary Fig. 17 | Body weights of mice vaccinated with mOVA-loaded C10, D6, or F5 LNPs.

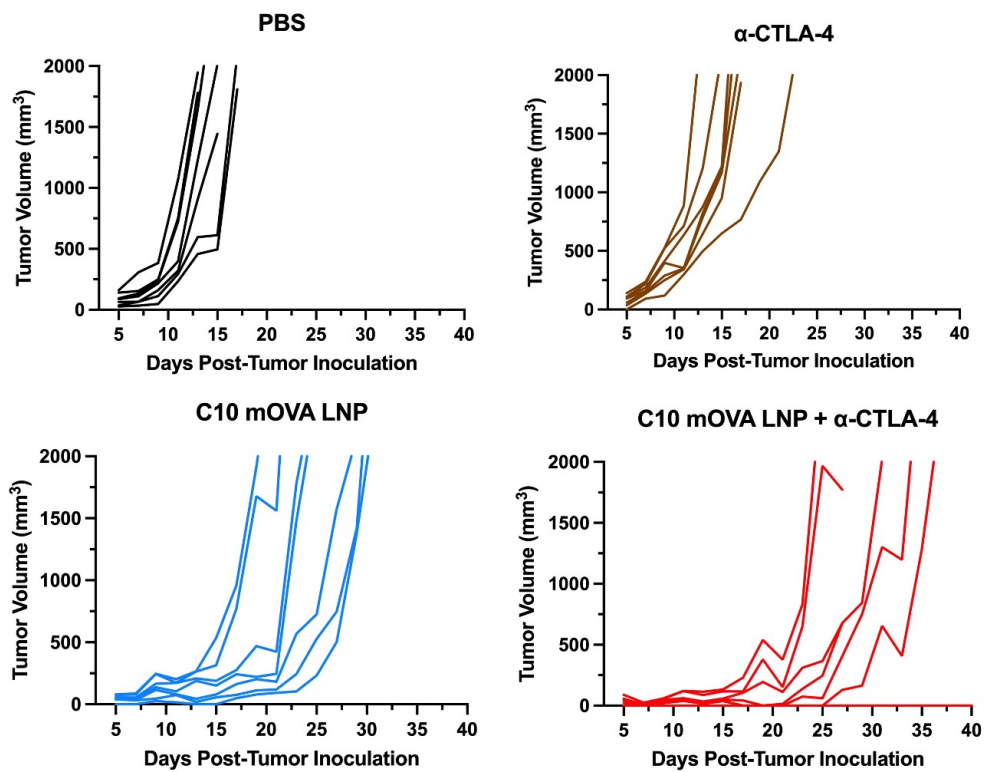
The body weights of mice were monitored during vaccination schedule. Mice are given three s.c. injections on day 0, 7 and 14 (10 μ g mOVA per injection). Data represent the mean \pm s.e.m. from a representative experiment (n = 6 biologically independent samples) of two independent experiments. Data on day 21 were analyzed using one-way ANOVA and Tukey's multiple comparisons test. NS, not significant.



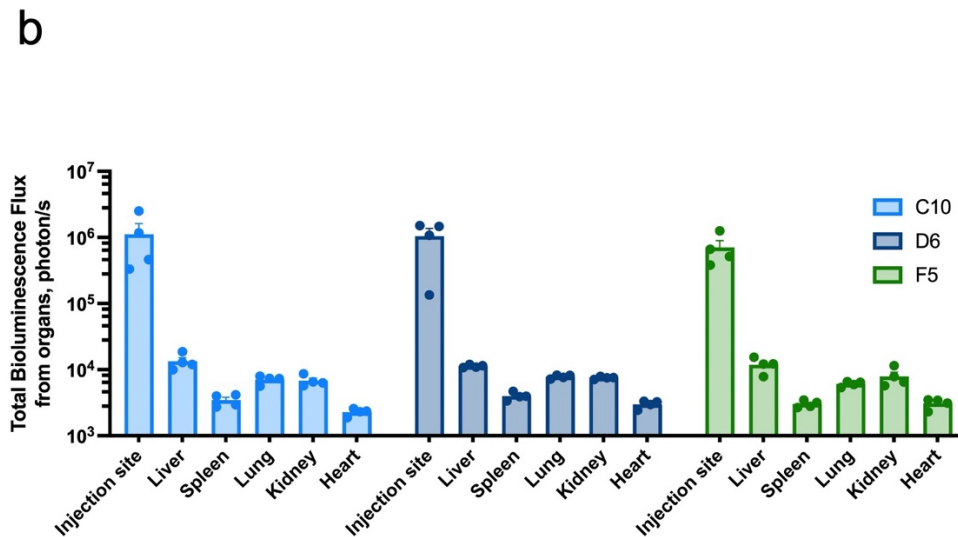
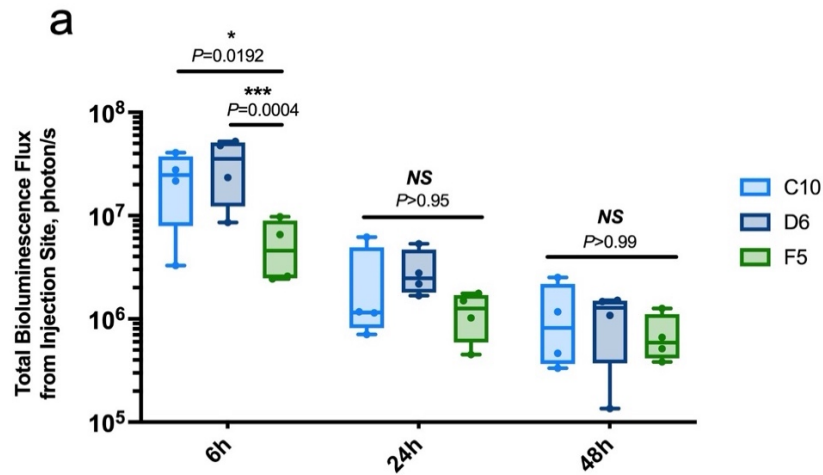
Supplementary Fig. 18 | Cytokine levels in blood serum samples collected on day 21 from mice vaccinated with different formulations. IL-6 (a), TNF- α (b), TGF- β (c), IL-12 (d), IFN- γ (e), IL-10 (f), and IL-4 (g) in blood serum on day 21 were determined by ELISA. Data represent the mean \pm s.e.m. from a representative experiment (n = 5 biologically independent samples) of two independent experiments. Data were analyzed using one-way ANOVA and Tukey's multiple comparisons test. NS, not significant.



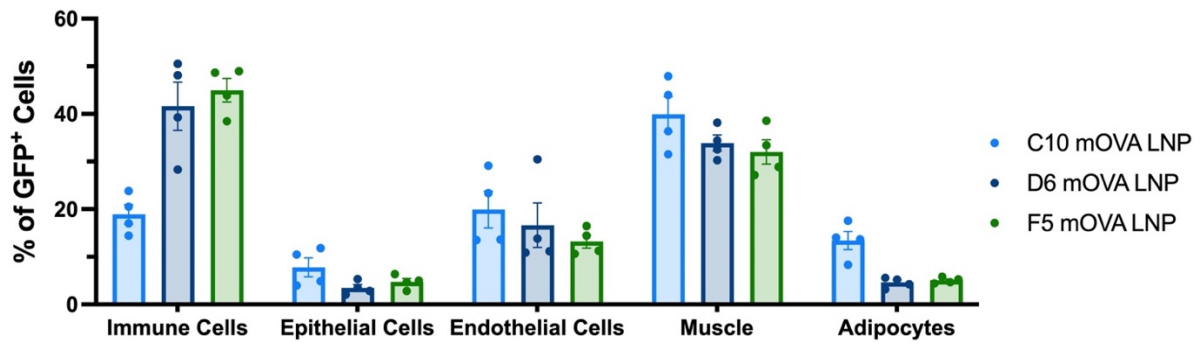
Supplementary Fig. 19 | Anti-tumor efficacy of top mRNA LNP formulations as therapeutic vaccines for MC38-OVA tumor model. Mice were inoculated *s.c.* with MC38-OVA cells and then given three *s.c.* injections, one week apart, of PBS or mOVA-loaded C10 (10 μg mOVA per injection). Two groups received a repeated anti-CTLA-4 monoclonal antibody (mAb; 100 μg per *i.p.* injection) treatment alone or in combination with the LNP treatment. Individual tumor volumes are shown over time.



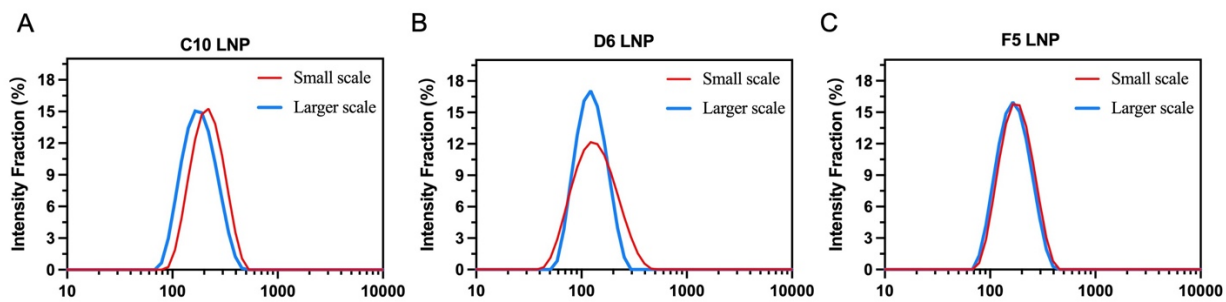
Supplementary Fig. 20 | Anti-tumor efficacy of top mRNA LNP formulations as therapeutic vaccines for EG7-OVA tumor model. Mice were inoculated *s.c.* with EG7-OVA cells and then given three *s.c.* injections, one week apart, of PBS or mOVA-loaded C10 (10 µg mOVA per injection). Two groups received a repeated anti-CTLA-4 monoclonal antibody (mAb; 100 µg per *i.p.* injection) treatment alone or in combination with the LNP treatment. Individual tumor volumes are shown over time.



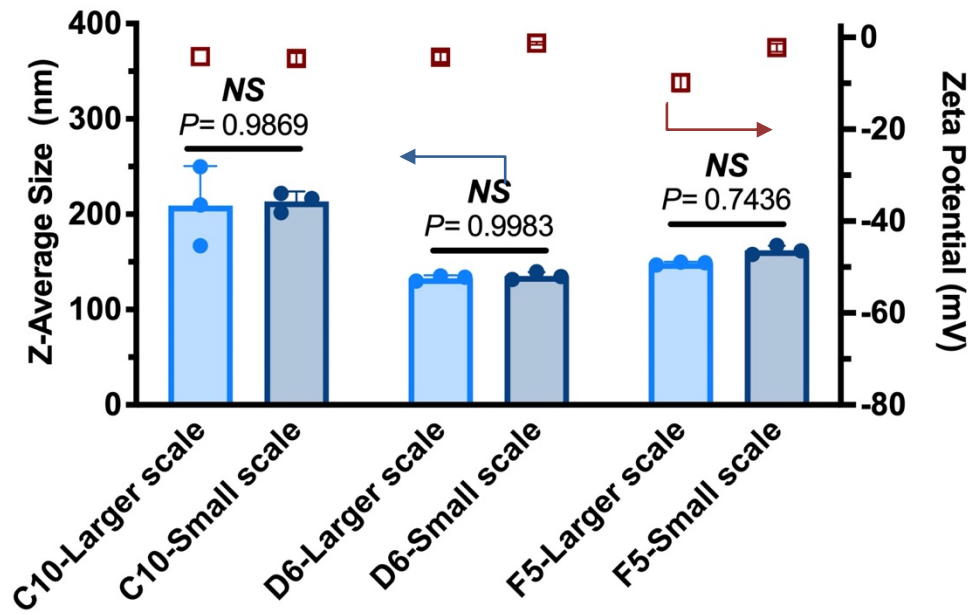
Supplementary Fig. 21 | *In vivo* transfection efficiency of LNP formulations in local injection site and major organs. In Vivo Imaging System (IVIS) was used to quantify the transgene level in the local injection site using luciferase encoding mRNA after administration of three LNP formulations C10, D6, and F5 at 6 h, 24 h, and 48 h (a). At 48 h, mice were sacrificed and the transfection levels in major organs were quantified (b). Data represent the mean \pm s.e.m. with $n = 4$ biologically independent samples. Statistical analysis was performed using two-way ANOVA followed by Tukey's multiple comparisons test. * $P < 0.05$, *** $P < 0.001$; NS, not significant.



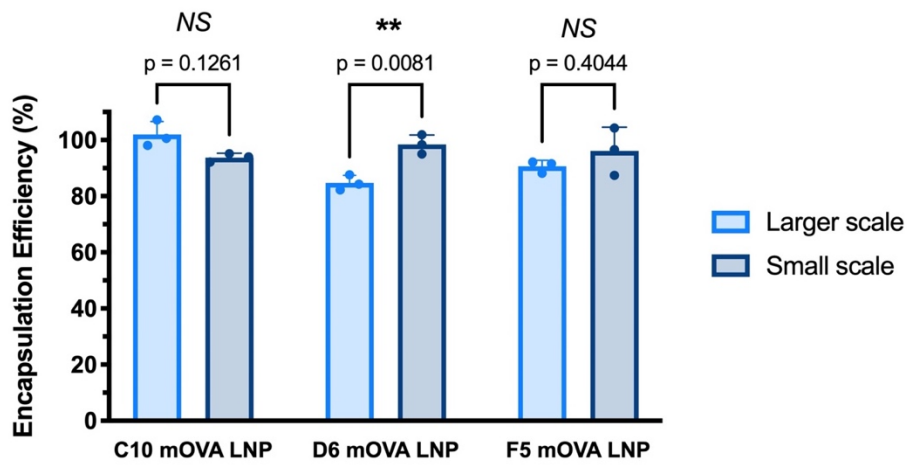
Supplementary Fig. 22 | Makeup of transfected cells at the injection sites of mice at 24 h post-treatment. Flow cytometry was used to quantify the percentage of specific cell types in the local injection site expressing GFP after vaccination of three GFP mRNA-loaded formulations C10, D6, and F5 including immune cells (CD45⁺), epithelial cells (CD326⁺), endothelial cells (CD31⁺), muscle cells (desmin⁺), adipocytes (CD45⁻CD31⁻CD36⁺). Data represent the mean \pm s.e.m. from a representative experiment ($n = 4$ biologically independent samples) of two independent experiments.



Supplementary Fig. 23 | Representative Z-average diameter distributions measured by Dynamic Light Scattering (DLS) of the top three mOVA LNP formulations synthesized via larger-scale and small-scale methods.



Supplementary Fig. 24 | Z-average size and zeta potential measurements measured by DLS of the top 3 mOVA LNP formulations synthesized via larger-scale and small-scale methods (n = 3). Z-average size was shown as mean ± S.D. on the left axis. Zeta potential was shown in cube with mean ± S.D at the right axis.



Supplementary Fig. 25 | Encapsulation efficiency assessments of the top 3 LNP formulations synthesized via larger-scale and small-scale methods. Encapsulation efficiency of LNPs containing OVA mRNA synthesized via larger-scale or small-scale methods were measured. Data are presented as mean \pm S.D. Data were analyzed using two-way ANOVA and Šidák's multiple comparisons test. ** $P < 0.01$; NS, not significant.

Supplementary Table 1 | Formulation details for the top 49 LNPs

Code ^a	Composition (Mol %) ^b				N/P Ratio ^e
	Hepler Lipid	DLin-MC3-DMA ^c	Cholesterol	DMG-PEG2000 ^d	
A1	30.00	30.00	39.92	0.08	12
A2	0.20	19.80	79.21	0.79	4
A3	10.00	10.00	79.21	0.79	8
A4	0.40	79.60	18.18	1.82	12
A5	30.00	30.00	36.36	3.64	8
B1	10.00	10.00	79.84	0.16	12
B2	30.00	30.00	36.36	3.64	8
B3	40.00	40.00	18.18	1.82	8
C1	10.00	10.00	79.84	0.16	4
C2	20.00	20.00	59.88	0.12	8
C3	0.78	39.22	59.88	0.12	12
C4	20.00	20.00	59.88	0.12	12
C5	30.00	30.00	39.92	0.08	4
C6	30.00	30.00	39.92	0.08	8
C7	30.00	30.00	39.92	0.08	12
C8	0.79	79.21	19.96	0.04	4
C9	7.27	72.73	19.96	0.04	4
C10	40.00	40.00	19.96	0.04	4
C11	0.10	19.90	79.21	0.79	4
C12	10.00	10.00	79.21	0.79	4
C13	0.20	39.80	59.41	0.59	12
C14	20.00	20.00	59.41	0.59	12
D1	20.00	20.00	59.88	0.12	8
D2	0.59	59.41	39.92	0.08	8
D3	30.00	30.00	39.92	0.08	12
D4	0.20	39.80	59.41	0.59	8
D5	0.40	39.60	59.41	0.59	8
D6	3.64	36.36	59.41	0.59	12
D7	20.00	20.00	59.41	0.59	12
D8	20.00	20.00	54.55	5.45	12
E1	10.00	10.00	79.84	0.16	12
E2	20.00	20.00	59.88	0.12	8
E3	20.00	20.00	59.88	0.12	12
E4	30.00	30.00	39.92	0.08	4
E5	30.00	30.00	39.92	0.08	8
E6	0.20	19.80	79.21	0.79	8
E7	0.78	39.22	59.41	0.59	4
E8	0.40	39.60	59.41	0.59	12
E9	1.18	58.82	39.60	0.40	4
E10	30.00	30.00	39.60	0.40	8
E11	1.57	78.43	19.80	0.20	4
E12	1.57	78.43	19.80	0.20	8
F1	10.00	10.00	79.84	0.16	8
F2	10.00	10.00	79.84	0.16	12

F3	20.00	20.00	59.88	0.12	8
F4	0.20	39.80	59.88	0.12	12
F5	5.45	54.55	39.92	0.08	8
F6	7.27	72.73	19.96	0.04	4
F7	1.18	58.82	39.60	0.40	8

Notes:

^aCode names A–F refer to different LNP formulations prepared using different helper lipids: Group A formulations were prepared with DOTAP as the helper lipid. Similarly, Groups B–F were prepared using DDAB, DOPE, DSPC, 14PA, and 18PG, respectively, as the helper lipid. DOTAP: 1,2-dioleoyl-3-trimethylammonium-propane; DDAB: dimethyl dioctadecyl ammonium; DOPE: 1,2-dioleoyl-sn-glycero-3-phosphoethanolamine; DSPC: 1,2-distearoyl-sn-glycero-3-phosphocholine; 14PA: 1,2-dimyristoyl-sn-glycero-3-phosphate; 18PG: 1-stearoyl-2-oleoyl-sn-glycero-3-phospho-(1'-rac-glycerol).

^bComposition for each formulation listed in the table refers to molar percent of all lipid components, excluding mRNA.

^cDLin-MC3-DMA: 4-(dimethyl amino)-butanoic acid, (10Z,13Z)-1-(9Z,12Z)-9,12-octadecadien-1-yl-10,13-nonadecadien-1-yl ester.

^dDMG-PEG2000: 1,2-dimyristoyl-rac-glycero-3-methoxypolyethylene glycol-2000.

^eN/P ratio refers to the molar ratio of total amount of nitrogen in ionizable lipid to total phosphate in mRNA.

Supplementary Table 2 | Formulation details and particle sizes for the top 7 LNPs

Code ^a	Composition (Mol %) ^b				N/P Ratio ^e	Z-Average size (nm) ^f	Polydispersity index (PDI) ^f
	Helper Lipid	DLin-MC3-DMA ^c	Cholesterol	DMG-PEG2000 ^d			
C3	0.78	39.22	59.88	0.12	12	164.8 ± 3.4	0.29 ± 0.05
C9	7.27	72.73	19.96	0.04	4	172.2 ± 5.4	0.18 ± 0.03
C10	40.00	40.00	19.96	0.04	4	208.9 ± 33.9	0.32 ± 0.06
D1	20.00	20.00	59.88	0.12	8	154.1 ± 2.8	0.27 ± 0.01
D2	0.59	59.41	39.92	0.08	8	145.9 ± 1.0	0.26 ± 0.06
D6	3.64	36.36	59.41	0.59	12	133.0 ± 2.3	0.28 ± 0.02
F5	5.45	54.55	39.92	0.08	8	148.6 ± 1.3	0.21 ± 0.04

Notes:

^aCode names C, D, and F refer to different LNP formulations prepared using different helper lipids: Group C, D, and F formulations were prepared with DOPE, DSPC, and 18PG, respectively, as the helper lipid. DOPE: 1,2-dioleoyl-sn-glycero-3-phosphoethanolamine; DSPC: 1,2-distearoyl-sn-glycero-3-phosphocholine; 18PG: 1-stearoyl-2-oleoyl-sn-glycero-3-phospho-(1'-rac-glycerol).

^bComposition for each formulation listed in the table refers to molar percent of all lipid components, excluding mRNA.

^cDLin-MC3-DMA: 4-(dimethyl amino)-butanoic acid, (10Z,13Z)-1-(9Z,12Z)-9,12-octadecadien-1-yl-10,13-nonadecadien-1-yl ester.

^dDMG-PEG2000: 1,2-dimyristoyl-rac-glycero-3-methoxypolyethylene glycol-2000, DMG-PEG 2000.

^eN/P ratio refers to the molar ratio of total amount of nitrogen in ionizable lipid to total phosphate in mRNA.

^fZ-average size (nm) and polydispersity index (PDI) were measured using dynamic light scattering method.